

# Mobility and Relaxation Determinations of Lithium in Lithium Aluminate Ceramics Using Solid-State NMR Spectroscopy

F. F. Stewart,<sup>\*,†</sup> J. F. Stebbins,<sup>\*,‡</sup> E. S. Peterson,<sup>\*,†</sup> Ian Farnan,<sup>‡</sup> S. O. Dunham,<sup>§</sup> E. Adams,<sup>§</sup> and P. W. Jennings<sup>§</sup>

Lockheed Idaho Technologies Company, Idaho National Engineering Laboratory, P.O. Box 1625, Idaho Falls, Idaho 83415; Stanford University, Department of Geology, Stanford, California 94305; and Montana State University, Department of Chemistry and Biochemistry, Bozeman, Montana 59717

Received August 29, 1994. Revised Manuscript Received November 17, 1994<sup>⊗</sup>

Lithium aluminate is one of the materials being considered for fusion reactor blankets. When preparing the ceramic, it is important to be able to monitor the microstructure since it is a controlling factor in the rate of tritium release from the blanket. Nuclear magnetic resonance spectroscopy (NMR) has been shown to be a useful tool for the nondestructive analysis of ceramics. Studies detailed in this paper include spectral acquisition, assignment, spin–lattice relaxation time measurements, temperature effects, their correlation to structure, and material purity. The ceramic of interest was lithium aluminate,  $\text{LiAl}_5\text{O}_8$ . This material was studied by observation of the NMR active nuclei  $^6\text{Li}$ ,  $^7\text{Li}$ , and  $^{27}\text{Al}$ . For these nuclei, spin–lattice relaxation times ( $T_1$ ) were measured and were found to vary considerably, correlating to the presence of paramagnetic impurities within the crystalline lattice. Previous research has shown that the coordination about the aluminum nucleus can be determined using  $^{27}\text{Al}$  NMR spectroscopy. Aluminum-27 NMR spectroscopy was successfully applied, and it provided valuable insight into composition of the ceramic.

## Introduction

There are two fusion blanket designs based upon lithium bearing ceramics: monolithic and sphere-pac. The sphere-pac, a bed of small ceramic spheroids, design offers several advantages including simple handling, thermal conductivity control, thermal stress control, and better cooling of the systems.<sup>1</sup> Thus, nondestructive analysis of materials is an increasingly important goal for both cost reduction and waste minimization. In this study, nuclear magnetic resonance (NMR) spectroscopy was applied to assess the ceramic solid phase and to quantitate the  $^6\text{Li}$ ,  $^7\text{Li}$ , and  $^{27}\text{Al}$  present in lithium aluminate ( $\text{LiAl}_5\text{O}_8$ ) spheres.

NMR studies conducted on lithiated glasses have revealed significant molecular motion of lithium within the glass. This is evidenced by sharpening of the resonance attributable for  $^7\text{Li}$  with increasing temperature.<sup>2–8</sup> Analogous mobility of lithium in ceramics is

a significant issue because rapid diffusion or volatilization during high temperature processing can lead to compositional variations within the material.  $^7\text{Li}$  NMR is a relatively straightforward technique used to observe diffusion and dynamics of lithium in a wide variety of materials including metals, silicates, borates, nitrides, sulfides, and halides in both crystalline and amorphous forms.<sup>9</sup> In many cases, the mobility of lithium results in significant reduction in peak widths with increasing temperature due to the onset of motional averaging of  $^7\text{Li}$ – $^7\text{Li}$  and other nuclear dipolar interactions.<sup>5</sup> This is generally accompanied by rapid decreases in the spin–lattice relaxation time  $T_1$ . Both peak narrowing and  $T_1$  data usually give activation energies in the range 30–80 kJ/mol. Many such studies have based detailed models of lithium diffusion on relaxation time measurements.

Studies of  $^6\text{Li}$  in solids, on the other hand, have been very limited because of its low natural abundance, relatively low NMR frequency, and long relaxation times, which make data collection quite time consuming. For example,  $T_1$  values as long as 830 s have been measured in aqueous solutions,<sup>10</sup> in contrast with typical values for  $^7\text{Li}$  of about 35 s.<sup>10</sup> Increasing temperature and fast lithium diffusion can lead to rapid decreases in  $^6\text{Li}$  relaxation times that are similar to those observed for  $^7\text{Li}$ , again with apparent activation energies on the order of 50 kJ/mol.<sup>11</sup>

The structure of  $\text{LiAl}_5\text{O}_8$  is related to the inverse spinel structure, with aluminum occupying a single type

<sup>†</sup> Idaho National Engineering Laboratory.

<sup>‡</sup> Stanford University.

<sup>§</sup> Montana State University.

<sup>⊗</sup> Abstract published in *Advance ACS Abstracts*, December 15, 1994.

(1) Turner, C. W.; Clatworthy, B. C. *Fabrication and Properties of Lithium Ceramics. Advances in Ceramics*, Hallenberg, G. W., Hastings, I. J., Eds.; American Ceramics Society: Washington, DC, 1990; Vol 27.

(2) Bray, P. J. NMR Studies of Glasses and Related Crystalline Solids. in *Magnetic Resonance*; Plenum Press, New York, 1970.

(3) Göbel, E.; Müller-Warmuth, W.; Olyschlager, H. *J. Magn. Reson.* **1979**, *36*, 371.

(4) Bishop, S. G.; Bray, P. J. *J. Chem. Phys.* **1968**, *48*, 1709.

(5) Hendrickson, J. R.; Bray, P. J. *J. Chem. Phys.* **1974**, *61*, 2754.

(6) Bray, P. J.; Gravina, S. J. *NMR Characterization in Glasses. Advances in Materials Characterization II*; Snyder, R. L., Condrate, R. A., Sr. Eds.; Plenum Press: New York, 1985; pp 1–29.

(7) Eckert, H.; Zhang, Z.; Kennedy, J. H. *J. Non-Cryst. Solids* **1989**, *107*, 271.

(8) Cocciantelli, J. M.; Suh, K. S.; Sénégas, J.; Doumerc, J. P.; Pouchard, M. *J. Phys. Chem. Solids* **1992**, *53*, 57.

(9) Stebbins, J. F. *Chem. Rev.* **1991**, *91*, 1353.

(10) Akitt, J. W. *The Alkali and Alkaline Earth Metals. Multi-nuclear NMR*; Mason, J., Ed.; Plenum Press: New York, 1987; p 190.

of tetrahedral site and lithium and aluminum occupying an octahedral site.<sup>12,13</sup> The phase formed at relatively low temperatures (below 1200–1300 °C) is thought to be nearly fully ordered into the lower symmetry  $P4_332$  space group, with most or all of the lithium in one type of octahedral site (with six octahedral aluminum neighbors) and a second octahedral site occupied by aluminum (with four octahedral aluminum and two octahedral lithium neighbors). There remains the possibility of some cation disorder depending on thermal history; mixing of lithium into tetrahedral sites and mixing of lithium and aluminum among octahedral sites are both possible. Although ranges in isotropic chemical shifts for  $^6\text{Li}$  and  $^7\text{Li}$  are known to be small,<sup>10</sup> analogy with sodium-23 shifts in silicates<sup>14</sup> suggests that large structural differences in oxide materials, such as coordination number change from four to six, should give measurable effects (at least 1 or 2 ppm).

Magic angle spinning (MAS)  $^{27}\text{Al}$  NMR has been shown to be a very useful technique for determining site occupancies and coordination numbers in a variety of solid oxide and silicate materials.<sup>15</sup> In particular, aluminum sites with four, five or six oxygen neighbors have distinct ranges of isotropic chemical shifts. In cases where quadrupolar coupling constants can be deduced from peak shapes, additional information can be gained about site symmetry. Disorder in the  $\text{LiAl}_5\text{O}_8$  structure could lead to extra  $^{27}\text{Al}$  NMR peaks or to changes in peak shape and intensity.

This work combines NMR of these three nuclides in a systematic analysis of  $\text{LiAl}_5\text{O}_8$  ceramics in order to assess  $^6\text{Li}$  content, purity, and dynamics and the overall structure of the material. We report relaxation time studies over a wide temperature range and describe shielding effects of conductive silicon carbide coatings on NMR spectra. Additionally, three separate lots of spheres were analyzed to provide a basis of comparison for deviations in composition and purity.

## Experimental Section

**Synthesis of Lithium Aluminate.** Lithium aluminate spheres used in this study were prepared by the method of Yang et al.<sup>16</sup> The samples were synthesized from lithium enriched to approximately 40% in  $^6\text{Li}$ . Three separate batches, termed A, B, and C, were synthesized and analyzed by NMR. Silicon carbide coatings of approximately  $32 \pm 3 \mu\text{m}$  thickness were applied using a proprietary CVD process.

**NMR Spectra.** Lithium-7 is a favorable spin  $3/2$  nucleus for study due to its large natural abundance, 92.5%, and its high nuclear receptivity (1500,  $^{13}\text{C} = 1$ ). Lithium-7 has a quadrupole moment,  $-4.5 \times 10^{-30} \text{ em}^2$  (unit of measurement for quadrupolar moments), which often can lead to broad signals. The  $^6\text{Li}$  nucleus, on the other hand, has a quadrupole moment that is 50 times lower, potentially giving narrower spectral lines. Narrowing of the signals potentially allows for resolution of differing lithium containing species. However, sensitivity is compromised due to low natural abundance

(7.5%) and significantly lower Larmor frequency and receptivity (3.58,  $^{13}\text{C} = 1$ ).

Room-temperature  $^7\text{Li}$ ,  $^6\text{Li}$ , and  $^{27}\text{Al}$  MAS NMR spectra were collected at 116.59, 44.146, and 78.172 MHz, respectively, using a Bruker AC-300P spectrometer operating at a field strength of 7.04 T. Samples were packed into 7 mm  $\text{ZrO}_2$  rotors and spun between 2 and 6 kHz using a Bruker supplied solid state accessory. Static experiments were conducted at the magic angle in the absence of spinning. Samples of the uncoated lithium aluminate spheres, approximately 800 mg, were generally studied using single pulses for all nuclei. The  $90^\circ$  pulses for the nuclei were determined for the aluminates using standard techniques and further characterization studies employed  $90^\circ$  acquisition pulse lengths. The  $90^\circ$  pulse lengths were determined for the lithium aluminate and were found to be 5.3 and 7.4  $\mu\text{s}$  for  $^7\text{Li}$  and  $^6\text{Li}$ , respectively. Delay times of 2–5 times  $T_1$  were found to be optimum to avoid saturation. Delays of 200 and 1800 s were utilized for  $^7\text{Li}$  and  $^6\text{Li}$ , respectively. A  $90^\circ$  pulse of 10  $\mu\text{s}$  was utilized in the DEPTH<sup>17</sup> sequence.

The elevated temperature  $^6\text{Li}$  studies (to 980 °C) were performed at 58.87 MHz on a Varian VXR-400S (9.4 T) spectrometer equipped with a nonspinning high-temperature probe. A boron nitride tube was used to contain approximately 1.48 g of sample. A longer  $90^\circ$  pulse width of 40  $\mu\text{s}$  was observed for this configuration. A  $\text{N}_2$ -5%  $\text{H}_2$  gas mixture was flushed through the probe during acquisition to prevent probe and sample oxidation at greatly elevated temperatures. Relaxation times were measured using the saturation–recovery technique.<sup>18</sup> Some  $^6\text{Li}$  MAS spectra were collected with this spectrometer using a Varian 7 mm MAS probe with spinning speeds of 4–6 kHz. Some  $^{27}\text{Al}$  MAS spectra were collected using a high-speed 5 mm probe from DOTY Scientific Inc. with spinning speeds up to 13 kHz, an NMR frequency of 104.5 MHz, and a pulse length of 0.5  $\mu\text{s}$  ( $15^\circ$  solid rf tip angle). These aluminum spectra were referenced to an acidified 1 M solution of  $\text{Al}(\text{NO}_3)_3$ .

Lower temperature studies were performed on a Bruker AM-500, 11.7 T field strength, spectrometer operating at 194.317 and 73.578 MHz for  $^7\text{Li}$  and  $^6\text{Li}$ , respectively. Samples were placed in  $\text{ZrO}_2$  rotors suited for a DOTY Scientific Inc. solids NMR probe.

**Elemental Analysis.** ICP-AES data were collected by the following procedure: 0.3 g of sample was placed in a platinum dish with 0.9 g of sodium tetrafluoroborate. This was fused in a muffle furnace at 1100 °C for 8 h followed by cooling to room temperature. The fusion product was then dissolved in 10 mL of concentrated nitric acid and 20 mL of deionized (Nanopure) water with gentle heating. The dissolved product was transferred to a 100 mL volumetric flask. The platinum dish was then rinsed with another acid/water mixture, and that was placed into the flask. The solution was allowed to cool and was diluted to volume. Analysis was performed using an ARL Model 3410 ICP-AES.

**X-ray Powder Diffraction Data.** X-ray powder diffraction data were obtained using a Phillips 1729 X-ray generator equipped with a copper anode. A Phillips 1710 powder diffraction goniometer was used for diffraction studies. Typical power settings were 40 kV and 20 mA; data were collected from  $10^\circ$  to  $85^\circ$  in  $2\theta$ . The powder samples were prepared by grinding about 0.5 g of the ceramic spheres to approximately –200 mesh. The samples were pressed into a 1  $\text{cm}^2$  sample holder and placed on the goniometer. Pattern matching was accomplished using the JANF X-ray diffraction data file.

## Results and Discussion

**$^6\text{Li}$  MAS NMR.** The sole feature of the  $^6\text{Li}$  spectrum for the ceramic was a sharp peak with no obvious quadrupolar coupling and line widths as low as 6.5 Hz. No spinning side bands were observed with spinning

(11) Brinkmann, D.; Mali, M.; Roos, J. In *Fast Ion Transport in Solids*; Vashishta, P., Mundy, J. N., Shenoy, G. K., Eds.; North-Holland: New York, 1979; pp 483–486.

(12) Braun, P. B. *Nature* **1952**, *170*, 1123.

(13) Famery, R.; Queyroux, F.; Gilles, J. J. *Solid State Chem.* **1979**, *30*, 257.

(14) Xue, X.; Stebbins, J. F. *Phys. Chem. Miner.*, in press.

(15) Engelhardt, G.; Michel, D. *High-Resolution Solid-State NMR of Silicates and Zeolites*; Wiley: New York, 1987.

(16) Yang, L.; Medico, R. R.; Baugh, A. Method for Producing Spherical Lithium Aluminate Particles; U.S. Patent No. 4 405 595, 1983.

(17) Bendall, M. R.; Pegg, D. T. *Magn. Reson. Med.* **1985**, *2*, 91.

(18) Fukushima, E.; Roeder, S. B. W. *Experimental Pulse NMR*; Addison-Wesley: Reading, MA, 1981.

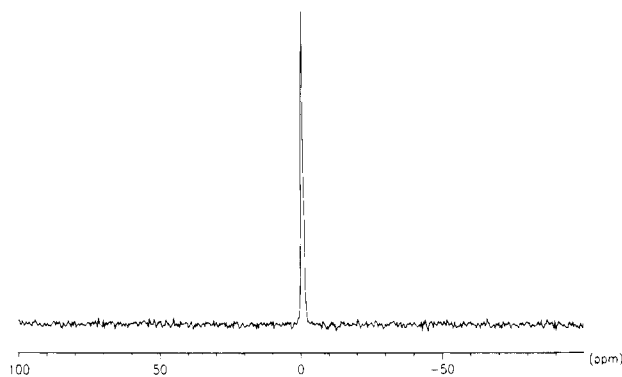


**Figure 1.**  $^6\text{Li}$  MAS NMR spectrum of lithium aluminate A taken using a single  $90^\circ$  pulse at a spinning speed of 4.8 kHz.

**Table 1. Effect of Temperature on the Signal-to-Noise Ratio<sup>a</sup>**

temp ( $^\circ\text{C}$ )	S/N ratio
ambient	55
180	30
780	3
980	6*

<sup>a</sup> 20 min acquisition, 1 s delay.

speeds above 1 kHz. The presence of a single resonance strongly suggests that all of the lithium in the structure has the same oxygen coordination number, and that there is no disorder between tetrahedral and octahedral sites (Figure 1). This is fully consistent with single crystal X-ray diffraction data.<sup>13</sup> However, the relatively small total range of lithium chemical shifts<sup>10</sup> means that more subtle structural effects, such as those that could be caused by disordering among nonequivalent octahedral sites, might not be detectable. Tests made by varying the amount of material within the MAS rotor indicate that the NMR signal is quantitative to within about 5%, if enough time is allowed for complete spin-lattice relaxation.

Elevated temperature experiments were conducted without spinning of the sample. Table 1 shows the observed signal to noise ratios for several different temperatures. All were one pulse experiments except for the data taken at 980  $^\circ\text{C}$ , which required 20 min of acquisition time with a 1 s delay between scans. Apodization of 200 Hz was applied to these data to enhance the signal-to-noise ratios.

Increasing the temperature had only a small effect on  $T_1$  values (Figure 2). There is some suggestion of a steeper slope above 200  $^\circ\text{C}$ , but uncertainties are relatively large. In any case, apparent activation energies derived from the data between ambient and 800  $^\circ\text{C}$  are only about 2–5 kJ/mol. This suggests that, unlike what is typical for  $^7\text{Li}$  (where stronger nuclear dipolar and quadrupolar couplings usually dominate), the relaxation mechanism for  $^6\text{Li}$  involves coupling to the electronic spins of paramagnetic impurities. In a rigid lattice, this typically results in weak variations with temperature.<sup>19</sup> The large values of  $T_1$ , as well as the large variation from one sample batch to another (Table 2) also indicate the role of impurities. Even with such a relaxation mechanism, however, rapid ionic diffusion is expected to result in much larger apparent

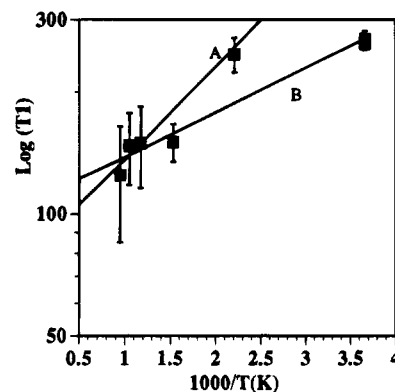


**Figure 2.** Arrhenius plot of  $^6\text{Li}$  spin-lattice relaxation times (in seconds) at high temperature. Uncertainties in high- $T$  data are estimated as being roughly  $\pm 20$  s, as shown. Solid lines illustrate the range of possible apparent activation energies: A for 4500 J/mol, B for 1800 J/mol.

**Table 2. Spin-Lattice Relaxation Measurements for Various Uncoated Samples**

$\text{LiAl}_5\text{O}_8$	temp ( $^\circ\text{C}$ )	$T_1$ (s)
A	ambient	$622 \pm 8$
B	ambient	$274 \pm 4$
B	180	$250 \pm 35$
B	380	$150 \pm 35$
B	580	$150 \pm 35$
B	680	$140 \pm 35$

activation energies.<sup>11,20</sup> From these data, we conclude that lithium is not highly mobile in this structure below 800  $^\circ\text{C}$ .

Comparison of the inversion-recovery  $T_1$  data collected under static and MAS conditions also restricts the possible relaxation mechanism. For example, the  $T_1$  for batch B measured at 58.9 MHz field strength under static conditions was  $262 \pm 8$  s, and with MAS, was  $274 \pm 4$  s. The similarity of these values indicates that dipolar interactions which would be averaged by spinning do not play a significant role in the relaxation mechanism. Therefore, under MAS conditions, we expect changes in  $T_1$  values to reflect spin diffusion to paramagnetic impurities. No other solid phases attributable to these metal impurities were observed in the X-ray powder diffraction pattern.

The presence of paramagnetic impurities was studied by ICP-AES (inductively coupled plasma-atomic emission spectroscopy). Table 3 details the largest concentrations of metal observed. The most significant metal is iron which is found to be most heavily concentrated in batch B with lower and similar amounts found for batches A and C. These relative concentrations are consistent with the  $^6\text{Li}$  relaxation measurements.

Silicon carbide coatings ( $32 \pm 3$   $\mu\text{m}$  thickness) were applied to the lithium aluminate spheres to study the effect of conductive coatings on NMR spectra. Lithium-6 was observed through the coating although the signal showed greatly reduced intensity. We propose two explanations for this behavior. The first possibility is shielding of the rf signal entering (and leaving) the sample by the coating. The second possibility is perturbation of the overall probe tuning caused by a large mass of conductor in the rf coil. The latter effect was observed as an approximately 7-fold reduction in the quality factor  $Q$ . This effect alone would decrease the

(19) Spearing, D. R.; Farnan, I.; Stebbins, J. F. *Phys. Chem. Mater.* **1992**, *19*, 307.

(20) Farnan, I.; Stebbins, J. F. *J. Am. Chem. Soc.* **1990**, *112*, 32.

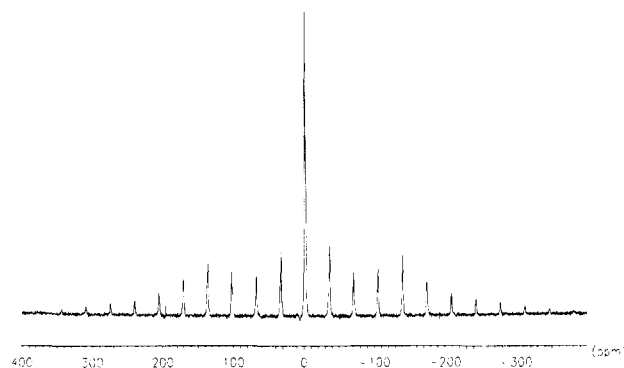


**Figure 3.**  ${}^7\text{Li}$  MAS NMR spectrum of lithium aluminate A using a single  $90^\circ$  pulse at a spinning speed of 4.0 kHz.

**Table 3.** ICP-AES Data

	metal		
	chromium (ppm)	iron (ppm)	manganese (ppm)
batch A	$12 \pm 2$	$104 \pm 12$	$<9.2$
batch B	$17 \pm 3$	$398 \pm 6$	$10 \pm 2$
batch C	$15 \pm 3$	$102 \pm 6$	$15 \pm 2$

rf field strength by a factor of  $7^{1/2}$ , or 2.6, predicting an increase in the  $90^\circ$  pulse width by a similar factor. We observed a change in the latter parameter from about 3 to 9  $\mu\text{s}$  for the uncoated and coated sample, suggesting that this effect is in fact significant. The reduced probe  $Q$  should also reduce the probe sensitivity by a factor of about 2.6. Accounting for analyzed  ${}^6\text{Li}$  contents and the mass of lithium aluminate in the rotor, the actual measured reduction in signal intensity from a coated sample was again about a factor of 3, consistent with the importance of this perturbation on the probe behavior. The spin-lattice relaxation time upon coating was also observed to increase from  $622 \pm 8$  s for the uncoated batch A to  $1130 \pm 409$  s for the coated batch A sample. The large margin of error in the  $T_1$  measurement for the coated sample was attributed to poor signal intensity, however, the magnitude of the value suggests possible loss of paramagnetic impurities during the CVD process.

**${}^7\text{Li}$  MAS NMR.** Lithium-7 NMR spectroscopy gives much more intense spectra than  ${}^6\text{Li}$ . The spectrum appears as a strong single resonance with spinning sidebands (Figure 3). Static spectra show the resonance with a broad Gaussian line shape with symmetrical quadrupolar coupling satellites. The quadrupolar coupling constant was measured at 43.1 kHz. Half-height line widths were found to be about 8000 Hz. Under MAS conditions, the half-height line widths were reduced to approximately 360 Hz.

The observation of a single resonance suggests a homogeneous distribution of lithium within the ceramic lattice. However, the half-height line width is large and could be masking slightly nonequivalent species. Spin-lattice relaxation times were measured by the inversion recovery method. A sharp transition was observed between negative and positive phases during the experiment suggesting a solitary  ${}^7\text{Li}$  species. A comparison of  $T_1$  measurements performed on batches A and B show similar changes as were observed for  ${}^6\text{Li}$ . The  $T_1$  measured for batch B was  $17.4 \pm 0.2$  s while batch A was  $32.2 \pm 0.6$  s. Further experiments were performed at both elevated and lowered temperatures. Spin-lattice relaxation studies performed on a third batch,

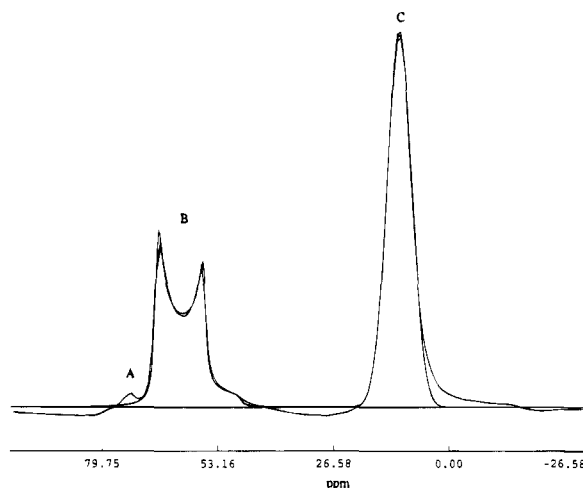


**Figure 4.**  ${}^{27}\text{Al}$  MAS NMR spectrum of  $\text{LiAl}_5\text{O}_8$ , showing central ( $\pm 1/2$ ) transitions only, and references to 1 M aqueous  $\text{Al}^{3+}$ . Collected at 104.5 MHz Larmor frequency and spinning speed of 13 kHz, with approximately  $15^\circ$  rf tip angle. Peak A is a combination of the central peak for a small amount of  $\text{LiAlO}_2$  impurity plus the center spinning side band of the  $\pm 1/2$  to  $\pm 3/2$  transition. Peak B is for the tetrahedral site in the  $\text{LiAl}_5\text{O}_8$ , with the fitted quadrupolar line shape; peak C is for the octahedral site, with a fitted Gaussian.

C, at 243 and 343 K did not differ significantly from each other (21 s at 343 K and 22 s at 243 K). These data support a single lithium species within the ceramic lattice that is rigidly held with minimal ionic diffusion.

Acquisition of  ${}^7\text{Li}$  spectra from the coated material suffers from the same difficulties observed for  ${}^6\text{Li}$ , specifically loss of signal intensity. Ideally, pulses may be selected such that the  $180^\circ$  pulse could be determined. Experimentally, the spectrum was observed to gain intensity up to the  $90^\circ$  pulse and then decrease to the null  $180^\circ$  pulse. Pulses of greater than  $180^\circ$  were consistently nulled, no negative signal was observed. One rationale is an rf gradient across the sample, some nuclei receive the designated excitation while others receive less excitation energy. The net result is scrambling of the observed resonances such that any received signal would appear nulled. To test for this scrambling effect, a pulse sequence entitled DEPTH<sup>17</sup> was used as an rf filter to screen all but the desired signals.

The DEPTH sequence selects out species that respond to a predetermined  $90^\circ$  pulse and filters out those that do not. The assumption employed is that all of the  ${}^7\text{Li}$  nuclei have the same  $T_1$ , independent of the applied field. Sorting of the resonances allows observation of a specific set of  ${}^7\text{Li}$  nuclei and the measurement of the relaxation time. Application of this sequence did give a  $T_1$  value of  $33.6 \pm 0.2$  seconds for batch A. A reduction in the relaxation time upon coating to  $8.1 \pm 0.1$  seconds was observed for batch A. These data differ from measurements taken for  ${}^6\text{Li}$ , presumably because of differing relaxation mechanisms.

**${}^{27}\text{Al}$  MAS NMR.** Because of its much greater chemical shift range,  ${}^{27}\text{Al}$  MAS NMR spectroscopy can potentially yield more structural information than either lithium nuclide. The spectrum for  $\text{LiAl}_5\text{O}_8$  is dominated by two main resonances (Figure 4). The lower frequency peak has a relatively narrow Gaussian shape (fwhm = 6.7 ppm) centered at 11.5 ppm when observed at 104.5 MHz. This position is consistent only with octahedral coordination. Analysis of the spinning side bands for

the satellite transitions of this peak allows us to estimate the isotropic chemical shift as 13.0 ppm with a quadrupolar coupling constant of  $1.7 \pm 0.2$  MHz. There is no indication of more than one octahedral aluminum site, even in the spinning side bands for the  $+^{1/2}-^{3/2}$  transition, for which second order quadrupolar broadening is much smaller than for the main  $-^{1/2}-^{1/2}$  peak. A second resonance at higher frequency can be well fitted by a quadrupolar doublet with a quadrupolar coupling constant of  $4.05 \pm 0.05$  MHz, an asymmetry parameter of  $0.0 \pm 0.1$ , and an isotropic chemical shift of  $70.5 \pm 0.5$  ppm. The latter value is compatible only with tetrahedral coordination. The uniaxial symmetry of the quadrupolar coupling is consistent with the published crystal structure.<sup>13</sup> A full manifold of spinning side bands for all five spin transitions are clearly observable, and their positions agree with this fit. The relative areas of the tetrahedral peak is  $39 \pm 2\%$  of the total area of both central transitions, again fully consistent with the ordered structure. The few percent disorder among Li and Al on the octahedral sites reported by Famery<sup>13</sup> is probably too small to be detected in our spectra.

One additional spectral feature is a weak resonance at 81.3 ppm. This is attributed to the central transition for  $\text{LiAlO}_2$ . Powder X-ray diffraction was performed as described previously. The major peaks were found to be  $\text{LiAl}_5\text{O}_8$ , with a small amount of  $\text{LiAlO}_2$  as well.

There is no obvious evidence for an alumina phase, but the major peaks of  $\gamma\text{-Al}_2\text{O}_3$  coincide almost exactly with some of the  $\text{LiAl}_5\text{O}_8$  maxima.

### Conclusion

Described in this paper is a multinuclear nondestructive approach to ceramic sphere analysis using nuclear magnetic resonance. Significant lithium transport was not observed for lithium aluminate as opposed to that observed previously in many glasses and ionic conductors. Spin-lattice relaxation measurements reflected the differences in relaxation mechanisms for each nuclide. Lithium-6 appears to relax most significantly through interactions with paramagnetic impurities, thus providing a possible measure for these impurities. On the other hand,  $^7\text{Li}$  is observed to relax much more strongly through dipole-dipole interactions. Further experiments using  $^{27}\text{Al}$  NMR provided the structural information necessary for evaluation of the ceramic. Taken together, these nuclear magnetic resonance methods represent a highly sensitive nondestructive analytic tool suitable for ceramic structural analysis.

**Acknowledgment.** The work described in this paper was supported by the United States Department of Energy through Contract DE-AC07-76IDO1570.

CM9404071